Available online at www.sciencedirect.com
SCIENCE DIRECT®
Applied Geochemistry 20 (2005) 1292–1308
Applied Geochemistry
www.elsevier.com/locate/apgeochem

# Application of tritium in precipitation and in groundwater of the Kouris catchment (Cyprus) for description of the regional groundwater flow

Anastasia Boronina [a,*], Philippe Renard [b,1], Werner Balderer [a,2], Willibald Stichler [c,3]

[a] *Institute of Geology, ETH Zürich, Switzerland*
[b] *Centre for Hydrogeology, University of Neuchâtel, Switzerland*
[c] *GSF-Institut of Hydrology, Neuherberg, Germany*

Received 27 May 2004; accepted 11 March 2005
Editorial handling by W.M. Edmunds
Available online 13 June 2005

**Abstract**

The Kouris catchment is located in the south of the Troodos massif in Cyprus. It constitutes one of the biggest catchments of the island with important freshwater resources. Geologically, the catchment includes an ophiolitic complex outcropping in the north which is overlaid by sedimentary rocks in the south. The hydrology is driven by a Mediterranean climate, a mountainous topography, and a complex distribution of the hydrogeological properties resulting from the complex geology.

To improve the understanding of groundwater hydrology of the Kouris catchment, 176 groundwater and precipitation samples were collected and their $^{3}H$ contents were analyzed. The three-dimensional $^{3}H$ transport in the groundwater was simulated by the PMPATH code. For numerical modelling, a regional input function of $^{3}H$ in precipitation was constructed from a linear regression between data for Cyprus and for neighboring meteorological stations. The calculated residence times for the groundwaters in the sedimentary aquifer and Pillow Lavas were greater than 48 a and were considerably greater than those of the ophiolitic complex (14–30 a). The calibrated aquifer porosities were in a range of 0.05–0.06. The PMPATH model was applied for delineation of spring catchments that were represented by quite narrow zones of lengths up to 5 km.

Another contribution resulting from the $^{3}H$ analysis was a better understanding of the river–aquifer interactions. In most of the southern part, the lithified sediments received only negligible amounts of water from the rivers, while the alluvial aquifer contained mostly water infiltrated from rivers. The largest springs in the southern part, associated with the alluvial aquifer, also discharged water identical to that in the rivers.


* Corresponding author. Present address: Hydrosciences UMR IRD-UMI&II-IRD, Case MSE, UMII, Place Eugène Bataillon, 34 095 Montpellier Cedex 5, France. Tel.: +33 4 67 14 90 46; fax: +33 04 67 14 47 74.
*E-mail addresses:* boronina@msem.univ-montp2.fr (A. Boronina), philippe.renard@unine.ch (P. Renard), Balderer@erdw.ethz.ch (W. Balderer), stichler@gsf.de (W. Stichler).
[1] Tel.: +41 32 718 26 90; fax: +41 32 718 26 03.
[2] Tel.: +41 1 633 27 43; fax: +41 1 633 11 08.
[3] Tel.: +49 89 318 725 66; fax: +49 89 318 733 61.

0883-2927/$ - see front matter © 2005 Elsevier Ltd. All rights reserved.
doi:10.1016/j.apgeochem.2005.03.007

## 1. Introduction

As a typical Mediterranean island, Cyprus experiences a scarcity of water resources. The ophiolitic mountainous complex that is exposed as an oval-shaped body in the center of the island (Fig. 1) is considered to be the most important groundwater reservoir for the country since it receives the largest amount of precipitation. The aquifer is fractured and strongly heterogeneous. Sustainable water management of the catchment requires an accurate understanding of the relations between surface and groundwater.

Tritium concentrations have often been applied to validate hydrological conceptual models. In many studies, $^3$H has been used as a groundwater dating tool (Stimson et al., 1996; Plummer et al., 2001; Marechal and Etcheverry, 2003). Commonly, the residence times are estimated by simulating the transport of $^3$H through an aquifer, knowing $^3$H input in precipitation, so that the simulated concentrations match the observed values. The simulation can be based either on simple conceptual-analytical models (lumped-parameter) or more complex numerical models.

The lumped-parameter, or box-models (Maloszewski and Zuber, 1982; Zuber, 1986; Maloszewski, 1996) imply distribution functions of several types (piston-flow, exponential, dispersion – the most common) allowing the transient input function of $^3$H contents in precipitation to be transformed into $^3$H concentrations in groundwater. The main advantage of these models is that only general geological knowledge (that might be descriptive) and measured $^3$H concentrations (to calibrate the models) are required for their use. The important disadvantage is the a priori assumption of a conceptual model or distribution function that can be rather complex and unknown in reality. Additionally, the dispersion model (associated with the most common behavior of hydrogeological systems) requires a dispersion coefficient, which is often not well known from field measurements. This leads to large uncertainties and non-uniqueness in residence time estimates.

An alternative approach for the interpretation of $^3$H data is numerical groundwater flow and transport modelling (see Konikow, 1996, for a review of models). Although, these models require additional parameters (which can be constrained by field measurements and observations) beside input and output concentrations, they result in a more complete description of the hydrogeological system. These methods allow not only obtaining residence times of groundwater (that are useful to make forecasts of groundwater contamination), but also testing the main conceptual assumptions underlying numerical models. The main drawback of these models is that they require a larger amount of input data and, consequently, they require more detailed studies. Additionally, a danger of over-parametrisation and the probability of non-uniqueness of a solution are well known intrinsic problems of numerical groundwater modelling.

Finally, both numerical and box-model estimates of residence times suffer from uncertainties resulting on the one hand from the uncertainty in the $^3$H input function, which is rarely available over the whole time period, and on the other hand from its non-uniqueness due to the bell shape of the input function.

The aim of this study is to use the information provided by $^3$H content in precipitation and groundwater in the Kouris catchment to test a regional hydrogeological conceptual model and to calibrate the corresponding transient numerical model.

Studies using $^3$H have been already conducted in Cyprus. From 1972 to 1978, an environmental isotope survey of Cyprus was sponsored and conducted by IAEA in

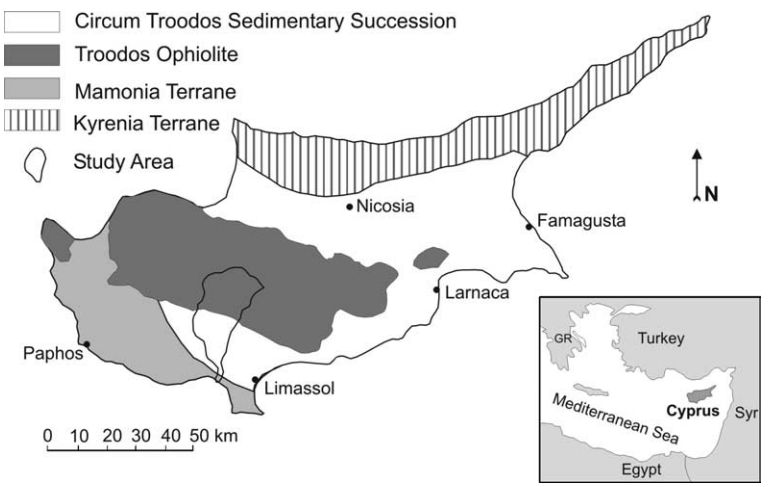


Fig. 1. Simplified geological map of Cyprus showing the location of the Kouris catchment.

collaboration with the Water Development Department (WDD) of Cyprus. The research carried out consisted of sampling environmental isotopes in springs, boreholes, and river baseflows originating from the Troodos Mountains. Additionally, snow and rainfall samples were analyzed for $^{3}H$. Despite a great number of analysis (more than 200 samples), the conclusions were quite uncertain due to the high geological heterogeneity and the large extent of the study area. The results of the survey were never published although they were integrated in a technical report (Jacovides, 1979). In the 1980s, an isotope survey was conducted on the sedimentary complex located west of Larnaka – approximately 30 km to the east of the Kouris catchment (Verhagen et al., 1991). Other studies were concentrated on the unsaturated zone of the sedimentary complex in the southeast of Cyprus in the Mesaoria area; those were related to the estimation of recharge from precipitation (Kitching et al., 1980).

In this paper, new $^{3}H$ data is integrated with those reported by Jacovides (1979) for the description of the hydrogeology of the Kouris catchment.

## 2. The Kouris catchment

The Kouris catchment is described in detail by Jacovides (1979), Afrodisis et al. (1986), and Boronina et al. (2003); in the present paper only the most essential information is provided.

The catchment extends from the Mediterranean Sea in the south to the top of the Troodos Massif in the north (Fig. 1). It covers an area of approximately 300 $km^2$. Elevations range from sea level to 2000 m within a distance of 30 km; local slopes in the Northern part rise up to 70%. Annual precipitation amounts increase from 300 mm along the coast to nearly 1200 mm in the Troodos Mountains, while mean annual potential evapotranspiration for the catchment is 1210 mm. The catchment is drained by the perennial rivers Kouris, Kryos and Limnatis (Fig. 2), fed by spring water during the "dry" season. The Kouris River is the largest in Cyprus with an average annual streamflow of 36 $Mm^3$ over the last 30 a. The catchment is divided into two main geological zones: an ophiolitic complex in the north and a sedimentary complex in the south unconformably overlying the ophiolites.

### 2.1. The ophiolitic complex

The ophiolites in Cyprus consists of ultramafic rocks, Gabbros, Sheeted Dykes and Pillow Lavas (Fig. 2). They are highly heterogeneous due to the presence of different lithological units, which are additionally fractured and altered at different scales. The transmissivities of the Gabbros and the diabase dykes vary from 2 to 703 $m^2$/day with a geometrical mean of 20 $m^2$/day according to the results of 40 pumping tests (Boronina et al., 2003). The Pillow Lavas are considered to have a low permeability at a regional scale, even if local zones of higher conductivity are likely to exist.

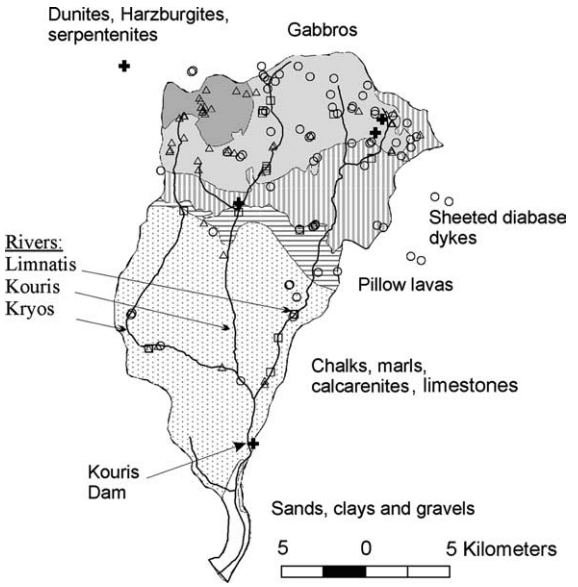


Fig. 2. Geological map of the Kouris catchment with sampling locations: crosses – precipitation; circles – boreholes; triangles – springs; squares – rivers.

There are a large number of springs that are associated with the plutonic and intrusive rocks; of those, 62 were documented; others (like many small springs in the north-eastern part of the Limnatis valley) could not be mapped individually. On the other hand, no springs were found discharging from the outcrops of Pillow Lavas.

The ophiolites contain the major groundwater resources of Cyprus; the water is stored in the fractured and altered zones of harzburgites, dunites, gabbros and diabases. The largest springs are exploited for drinking and irrigation water supply of nearby villages (springs Archolochania – average discharge of 31 L/s, Loumata "B", "Loumata "C") and tourist center "Troodos" (springs Troodos A, B, C).

### 2.2. The sedimentary complex

The sedimentary complex is composed essentially of lithified sediments (chalk, marls, calcarenites, limestones) – (Fig. 2) and unconsolidated alluvium deposited in the river valleys.

The water resources of the lithified sediments are poor due to low effective precipitation and low transmissivity (regional value is around 3 $m^2$/day); additionally, the groundwater has salt contents up to 1 g/L – higher than those in the ophiolitic aquifer.

Table 1
Types, number and $^{3}H$ contents of water samples, analyzed for $^{3}H$ in 1998–2002 and in 1960–1978 (Jacovides, 1979), http://isohis.iaea.org

| | 1972–1978 (ground- and surface water), 1960–1974 (precipitation) | | | | 1998–2002 | | | |
|---|---|---|---|---|---|---|---|---|
| | Number of samples | Number of sampling points | Range of $^{3}H$ concentrations (TU) | Average $^{3}H$ concentrations (TU) | Number of samples | Number of sampling points | Range of $^{3}H$ concentrations (TU) | Average $^{3}H$ concentrations (TU) |
| Rainfall samples | 64[a] | 1 | 14–2300 | | 12 | 3 | 2.8–4.3 | 3.5 |
| Rivers | 3 | 3 | 31.8–37.4 | 34.3 | 43 | 12 | 2.7–8.6 | 4.5 |
| *Spring samples* | | | | | | | | |
| Ophiolitic complex (ultramafic rocks, gabbros, diabase dykes) | 26 | 14 | 10.0–61.5 | 34.9 | 56 | 27 | 2.1–32 | 9.7 |
| Alluvium aquifer | 1 | 1 | – | 46.1 | 7 | 5 | 2.6–18.5 | 6.1 |
| *Borehole samples* | | | | | | | | |
| Ophiolitic complex (ultramafic rocks, gabbros, diabase dykes) | 43 | 21 | 0.6–62.0 | 26.0 | 34 | 31 | 1.5–22.5 | 7.5 |
| Ophiolitic complex (Pillow Lavas) | 4 | 3 | 0.02–3.5 | 1.0 | 7 | 4 | 1.0–4.4 | 1.6 |
| Sedimentary complex | – | – | | | 7 | 5 | 0.7–3.1 | 1.8 |
| Alluvium aquifer | – | – | | | 10 | 8 | 3.2–10.2 | 5.8 |
| Total | 141 | 43 | | | 176 | 95 | | |

[a] Sixty four rainfall samples were collected in 1960–1974 for the Prodromos meteostation by IAEA in a collaboration with WDD, analyses are included in the GNIP database (http://isohis.iaea.org).

Water occurrence is sporadic – from 73 recorded boreholes, drilled in the sedimentary complex in the 1970–1990s for irrigation purpose, 70% were unsuccessful for water exploitation.

The unconsolidated sediments consist of sands, gravels, and boulders. These alluvial aquifers are narrow, sometimes less than 50 m in width, and discontinuous, although they contain a very important groundwater resource for the southern part of the catchment.

Five main springs of the southern part associated with the alluvial aquifer are located in the river valleys. The instantaneous discharge of one of the largest monitored springs (Mavromata) has varied from 0.65 to 215 L/s over the last 50 a. Other springs in the river valleys were found in the outcrops of lithified sedimentary rocks. They are usually comparatively highly mineralized (up to 1600 mg/L) and have small discharges (less than 1 L/s).

## 3. Collection of water samples and uncertainties of measurements

For the present study, 176 groundwater, surface water, and precipitation samples from 95 locations were collected and analyzed for $^{3}H$ and major ions – the analyses were included partly in the diploma theses of Moll (2000), Steiner (2000) and Jorin (2001). Samples were collected in different seasons during the years 1998–2001 to investigate the temporal variability of $^{3}H$ concentrations (see Table 1 and Fig. 2 for details).

For the $^{3}H$ content in precipitation in Cyprus, 76 measurements were used from two main sources: (a) 12 new samples collected in 2000–2001 in Agros (N: 3,863,800 m, E: 501,300 m, altitude: 1015 m), at the Kouris Dam (N: 3,842,500 m, E: 493,000 m, altitude: 220 m), and in Saittas (N: 3,858,300 m, E: 492,000 m, altitude: 640 m); (b) 64 analyses from the IAEA network (http://isohis.iaea.org) sampled in 1960–1974 in Prodromos (N: 3,868,300 m, E: 484,200 m, altitude: 1380 m).

For the $^{3}H$ distribution in groundwater, 77 earlier measurements (Jacovides, 1979) were used in addition to the samples collected for the present study.

The analytical errors ($2\sigma$) were 0.7–2.0 TU (1 TU = 0.118 Bq/L); the higher values pertained to the samples taken in the late 1970s.

## 4. Tritium content in precipitation

The meteorological station in Prodromos (1380 m a.s.l., 2 km NE from the Kouris catchment) was selected as a representative location for the description of $^{3}H$ content in the precipitation over the catchment. This station has monthly records from 1960 to 1974 (http://isohis.iaea.org). The measurements have a high positive linear correlation (with a coefficient 0.99) with the data from the meteorological station located in Nicosia.

Table 2 presents the results of a linear correlation analysis between the data from Prodromos and those from the 5 meteorological stations, located at latitudes close to that of Prodromos. The meteorological station in Ottawa (Canada) was included in Table 2 because it was the only station where $^{3}H$ content in precipitation was measured before 1960. The comparative analysis of linear correlations was based on 27 monthly values between December 1963 and March 1974 since only for that period were the data recorded at all meteorological stations.

Finally, for 1953–1960, the input function for $^{3}H$ in precipitation at Prodromos was constructed on a linear regression with data from Ottawa since it was the only place for that period where $^{3}H$ was measured in precipitation. For the years 1963–1976, $^{3}H$ data from Prodromos were used. For other years meteorological stations were chosen where linear regressions with data from Prodromos for the period December 1963–March 1974 were the best and where measurements for requested periods were available. Thus, from Table 2, an optimal input function for $^{3}H$ had to be based on the data from Athens for 1960–1962 and 1976–1991 (correlation coefficient 0.92 for the years 1963–1974) and from

Table 2
Correlation between $^{3}H$ concentrations in monthly lumped rainfall samples from the selected meteorological stations

| Location | Latitude | Longitude | Period of measurements | Coefficient of linear correlation with $^{3}H$ content in Prodromos | |
|---|---|---|---|---|---|
| | | | | Arithmetic | Logarithmic |
| Ottawa (Canada) | 45°19′12″ | 75°40′12″ | 1953–1999 | 0.86 | 0.88 |
| Antalya (Turkey) | 36°52′48″ | 30°42′0″ | 1963–1999 | 0.73 | 0.90 |
| Ankara (Turkey) | 39°57′00″ | 32°52′48″ | 1963–1999 | 0.98 | 0.93 |
| Bet Dagan (Israel) | 32°00′00″ | 34°49′12″ | 1960–1999 | 0.86 | 0.91 |
| Alexandia (Egypt) | 31°11′00″ | 29°57′00″ | 1961–1989 | 0.98 | 0.85 |
| Athens (Greece) | 37°54′00″ | 23°43′48″ | 1960–1991 | 0.99 | 0.94 |

Ankara for 1992–1999 (correlation coefficient 0.87 for the years 1963–1974). The actual $^3$H concentrations were used for the 1950s, while for later periods the logarithms of the concentrations were used in order to smooth the influence of large values in the 1960s on the $^3$H concentrations predicted for the 1980–1990s.

The regression equations to calculate the $^3$H content of monthly precipitation in Prodromos were the following:

$$C_P = -1.393 + 0.587C_O \quad \text{for 1953–1960,} \tag{1}$$

$$\mathrm{LN}(C_P) = 0.83 + 0.82\mathrm{LN}(C_{Ath}) \quad \text{for 1960–1962 and 1976–91,} \tag{2}$$

$$\mathrm{LN}(C_P) = 0.20 + 0.82\mathrm{LN}(C_{Ank}) \quad \text{for 1992–1999,} \tag{3}$$

where $C_P$ and $C_O$, $C_{Ath}$, and $C_{Ank}$ represent, respectively, the monthly averaged $^3$H contents in precipitation at Prodromos, Ottawa, Athens, and Ankara. Average relative uncertainties of the approximations were calculated as:

$$\sigma = \frac{\sum \sqrt{\left(\frac{C_P\mathrm{obs}_i - C_{P_i}}{C_{P_i}}\right)^2}}{N}, \tag{4}$$

where $C_P\mathrm{obs}_i$ and $C_{P_i}$ represent the observed and calculated $^3$H concentrations in the Prodromos precipitation for a time period $i$. Eq. (4) provides the following uncertainty estimates: $\sigma = 0.5$ – for 1953–1960; $\sigma = 0.3$ – for 1960–1962 and 1976–1991; $\sigma = 0.3$ – for 1992–1999.

Finally, the annual $^3$H contents in precipitation at Prodromos were reconstructed (Fig. 3) from the estimated (Eqs. (1)–(3)) and the measured monthly $^3$H concentrations, averaged for the rainy seasons (October–March). The dashed lines in Fig. 3 represent the range of uncertainty according to the calculated $\sigma$ (Eq. (4)). For the years 1963–1976, the data corresponded to samples from Prodromos and the uncertainty was estimated to be $\sigma = 0.1$ (mean calculated relative error of the measurements in the laboratory). Additionally the values obtained in the Kouris catchment (Agros village) in November and December 2000 were incorporated into the input function with a measurement uncertainty of 0.7 TU.

## 5. Tritium content in surface and groundwater

### 5.1. Surface water

The $^3$H contents in the rivers in the "dry" seasons were quite spatially uniform (Table 1): 31.8–37.4 TU in 1978 and 2.7–8.6 TU in 1998–2002. These values were similar to average $^3$H concentrations in springs of the ophiolitic complex. During rainfall events, in the years 2000–2001, the $^3$H content of the rivers were lower due to surface runoff. However, hydrograph separation using $^3$H data was not possible because most of the signals were in the range of measurement uncertainties.

### 5.2. Groundwater

#### 5.2.1. Ophiolitic complex

The average $^3$H content of the groundwater discharging from springs of the ophiolitic complex (Table 1), indicated the presence of anthropogenic $^3$H. In the rainy season, springs were normally discharging a considerable amount of surface water originating from recent rainfalls (Fig. 4) which coincided in the time period with maximum discharge rates. Those springs might consequently be endangered by surface pollution. Some springs in Agros and Agious Theodorous villages are already not suitable for drinking due to petrol and sewage contamination.

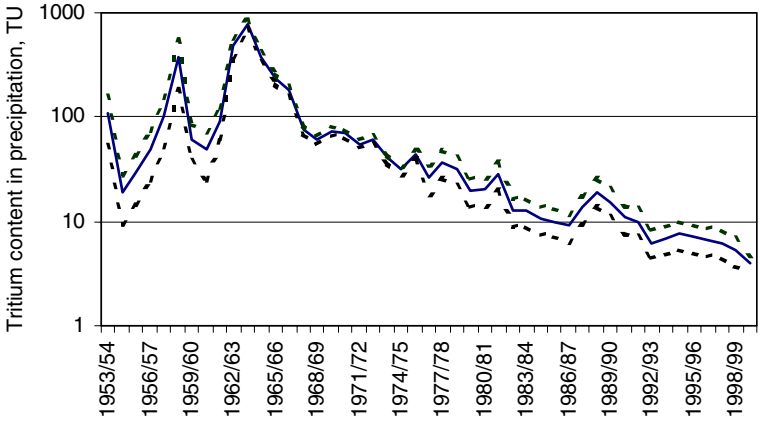


Fig. 3. Input function for $^3$H content of the precipitation over the Kouris catchment. Dashed lines limit the range of the uncertainty.

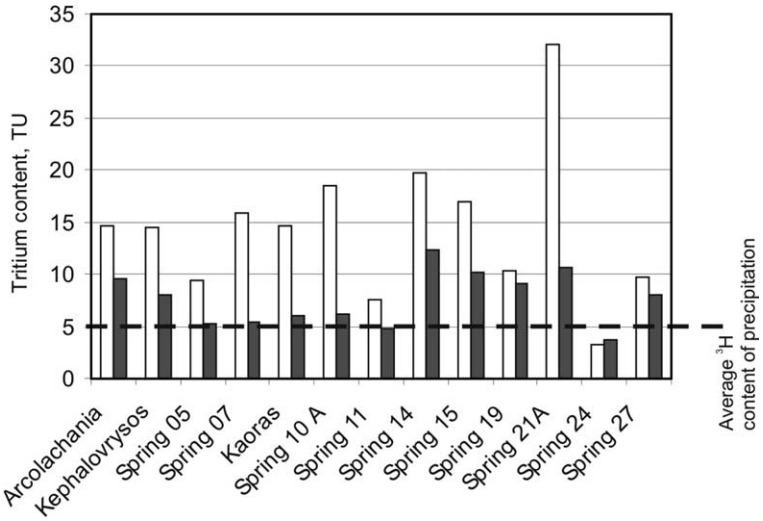


Fig. 4. Tritium contents of groundwater, discharging from the selected springs of the ophiolitic complex in 1998–1999: open bars – dry seasons; filled bars – wet seasons.

The $^3$H contents in boreholes were highly variable. They indicated that the groundwaters could be infiltrated from less than 10 a ago (30–60 TU in 1976–1978 for boreholes 19/76, 57/76, 30/76) to more than 45 a ago (less than 1.5 TU in 2000 for boreholes v2/94, w215/90, 146/90). Seasonal changes were not systematic; they depended rather on the pumping regime. The boreholes heavily pumped during a "dry" season (typically for irrigation) eventually yielded water that was older than 45 a, indicating extraction from old groundwater reservoirs. Such water is not renewable rapidly.

*5.2.2. Volcanogenic rocks*

The aquifer in the volcanogenic rocks (Pillow Lavas) is confined and located at a depth of more than 100 m, with no springs observed. The $^3$H data from 1976–1978 and 1998–2002 showed that the aquifer contained water, mainly infiltrated before 1953 (Table 1).

*5.2.3. Alluvial aquifer*

The $^3$H contents of the groundwaters in the alluvium were similar to those of the streamwaters (Table 1). In a "dry" season, it was a mixture of discharges from different ophiolite springs. In the rainy season, the water originated additionally from surface runoff. These facts are in an agreement with results of stable isotopes and hydrochemistry studies (Boronina et al., 2005b) concluding that the alluvium aquifer was fed by the streamwater, both in "dry" and "wet" seasons, rather than by the groundwater of the sedimentary aquifer. The biggest springs in the southern part of the catchment, located in the river valleys, were discharging groundwater with $^3$H contents identical to those in the rivers and the alluvium aquifer. The ophiolitic signature of groundwater in the alluvial aquifer and in the biggest springs of the southern part of the catchment supported the idea that most of the water resources of the whole catchment originate from the north of the region, within the ophiolitic aquifer.

*5.2.4. Sedimentary aquifer (consolidated)*

From 7 oreholes sampled in the consolidated sediments, 3 had $^3$H concentrations less than 0.8 TU in 2002, corresponding to residence times more than 48 a. The remaining 4 boreholes contain $^3$H contents of (2.3–3.1) ± 0.7 TU that could equally correspond to "old" water or to recent precipitation (last 2–3 a). Comparatively high amounts of $NO_3$ (more than 50 mg/L in two boreholes) usually coinciding with the application of fertilizer to crops, supported the idea of a "young" age of water. However, this might have been due to direct infiltration of irrigation water around the borehole casing. On the other hand, existence of "old" water (less than 1 TU in 1984 – Verhagen et al., 1991) in the same kind of rocks 30 km to the east of the Kouris catchment, supported the hypothesis of high groundwater residence times in the sedimentary rocks of Cyprus.

In the vicinity of the rivers, the groundwater discharging from small springs at the outcrops of the consolidated sedimentary rocks contained 0.8 ± 0.7 TU of $^3$H that differed from the $^3$H composition of the streamwater (3–4 TU in the years 2000–2002). This indicates that, first, there was no significant infiltration from the rivers, and, second, those sediments contained groundwater infiltrated more than 48 a ago, before the atmospheric $^3$H peak.

## 6. Transient groundwater flow model

The aim of this model was to test the validity of the hydrogeological model previously established and discussed (Boronina et al., 2003). The question was, whether the $^3$H transport in the aquifer could be simulated so that there was a reasonable agreement between observed and simulated $^3$H contents.With this purpose in mind, a prerequisite was to extend the previous 2D regional steady-state model (Boronina et al., 2003) into a transient 3D model so that it could on the one hand reproduce the transient baseflow and piezometric annual variations, and on the other hand allow the calculation of the velocity field for the $^3$H transport in the aquifer. The simulations were performed with MODFLOW (Harbaugh and McDonald, 1996; Chiang and Kinzelbach, 2001).

### 6.1. Time-independent parameters

The model grid previously established (Boronina et al., 2003) was refined to equal cell sizes of 125 by 125 m. The aquifer was discretized vertically into 4 layers. The two upper layers corresponded to the unsaturated zone in order to model $^3$H delay.The two lower layers represented the aquifers. The rivers and springs were imposed as boundary conditions in the third layer (counting from the top). All layers were modelled as being confined. Indeed, drilling records in the ophiolites indicated that the aquifer was normally confined. The two upper layers were also simulated as a confined aquifer allowing modelling a downward $^3$H transport via an unsaturated zone of a fixed thickness.

The total transmissivities were kept identical to those of the steady-state model (Fig. 5) and were distributed vertically between the two lower layers of the aquifer. For the two upper layers, a vertical hydraulic conductivity was set to 0.1 m/day for the first upper layer (soils) and 0.5 m/day for the second layer (fractured ophiolites and sediments) while the horizontal hydraulic conductivity was assumed to be negligibly small in order to model only vertical flow in the unsaturated zone.

External and internal boundaries and input parameters for River and Drain packages were transferred from the steady-state model (Fig. 5) and slightly modified during calibration.

### 6.2. Time-dependent parameters

The modelled period extended from 1978 to 1999. It was discretized into 21 regular time steps of 365.25 days each. The most complete input and calibration data set was available for the years 1984–1999, consequently model constraints were based on that period.

The yearly recharge during the period 1984–1999 was calculated by the following balance equation:

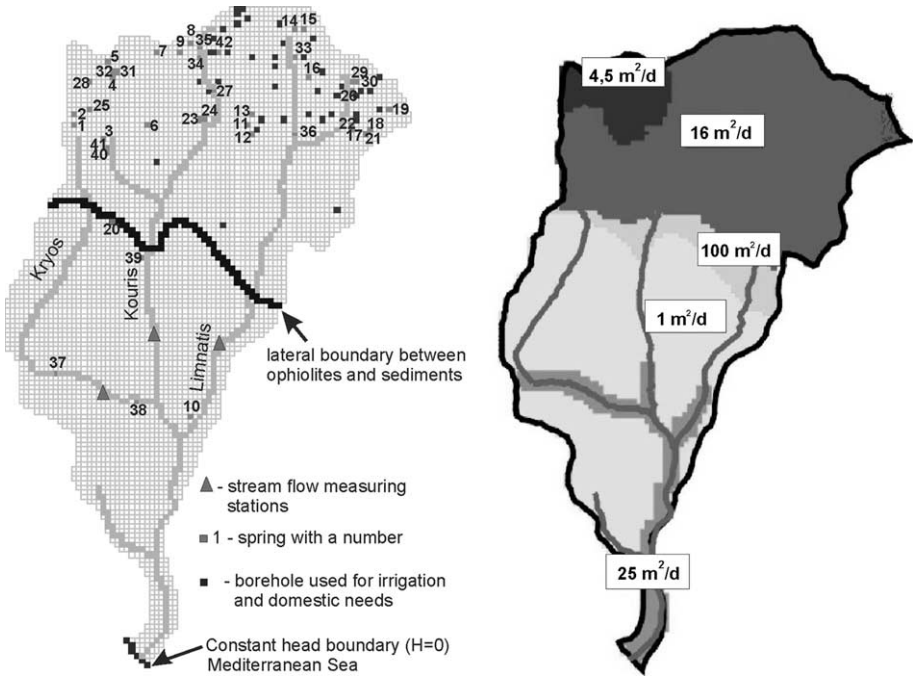


Fig. 5. Plan view of time-independent input parameters for the transient groundwater flow model: (left) boundary conditions (springs, rivers and boreholes are associated with the third layer); (right) areal transmissivity zonation (absolute values refer to the sum of transmissivities of the third and the fouth layers).

$$\text{Recharge} = \text{Rainfall} - \text{Actual evapotranspiration–surface runoff} + \text{Changes in groundwater storage} \quad (5)$$

The *Average Actual Evapotranspiration* (AvAcEv) for 1984–1999 was estimated as

$$\text{AvActEv} = \left(\sum^{15\ a}\text{Rainfall} - \sum^{15\ a}\text{Streamflow} - \sum^{15\ a}\text{Water demands}\right) \Big/ 15\ \text{a},$$

$$\text{AvActEv} = 184.6\ \text{Mm}^3/\text{a} \quad (6)$$

The *Actual Evapotranspiration* was assumed to be uniform for all years and equal to the *Average Actual Evapotranspiration* (Eq. (6)). This assumption was based on the fact that potential evapotranspiration estimated by the modified Penmann equation was almost constant through the years (Boronina et al., 2003). However, the authors admit that this assumption has serious limitations in a semi-arid climate where actual evapotranspiration is highly dependent not only on climate, but also on the amount of water available in the soil. This is why, during the model calibration, the input recharge had to be further corrected: it was reduced for the years with high amounts of annual precipitation and increased for very "dry" years.

*Surface runoff* was estimated by hydrograph separation with fixed- and sliding interval methods (Pettyjohn and Henning, 1979; Sloto and Crouse, 1996).

The values of all the variables in Eq. (5) are summarized in Table 3 (columns II, III, IV). In column IV ("recharge-changes in groundwater storage"), positive values indicate occurrence of recharge while negative ones are related to a decrease of groundwater storage due to excess of total evapotranspiration.

Columns V and VI show, respectively, total water demands and total baseflows, separated from river hydrographs (Boronina et al., 2003). [Estimates of baseflow were crucial for the groundwater model and their accuracy was linked directly to an accuracy of the model forecasts. However (and it is explained by Boronina et al., 2003), it was not possible either to quantify uncertainties of curve-fitting methods (Pettyjohn and Henning, 1979; Sloto and Crouse, 1996) or to obtain data necessary for other methods.]

Averaging recharge values (positive changes in column IV of Table 3) results in an annual amount of 38.4 $Mm^3$, which is equal to 17% of the average annual rainfall (223.0 $Mm^3$). This percentage is in an agreement with the results of an evaluation of the recharge based on the $Cl^-$ mass-balance method applied earlier for the same area (Boronina et al., 2003).

For the years 1978–1983, the estimates of input recharge and evapotranspiration were more uncertain due to the absence of streamflow measurements. Thus, calculations were based on a linear relationship between rainfall and recharge (evapotranspiration) that was derived for the period 1984–1999 (Fig. 6)

$$\text{Recharge(evapotranspiration)} = 0.92 \times \text{Rainfall} - 184.2,$$

where recharge/evapotranspiration and rainfall corresponded, respectively, to columns IV and II of Table 3. This relationship was used to calculate the input rate of recharge or evapotranspiration from

Table 3
Components of water balance for the Kouris catchment, used for transient groundwater modelling, $Mm^3$ per hydrological year

| Hydrological year I | Rainfall II | Surface runoff III | Recharge-changes in groundwater storage IV | Water demand V | Baseflow VI |
|---|---|---|---|---|---|
| 1984/1985 | 234.0 | 9.6 | 39.8 | 8.1 | 29.9 |
| 1985/1986 | 174.8 | 3.8 | −13.7 | 8.3 | 11.7 |
| 1986/1987 | 293.8 | 11.2 | 98.0 | 8.3 | 39.8 |
| 1987/1988 | 286.2 | 17.4 | 84.1 | 8.6 | 52.4 |
| 1988/1989 | 242.2 | 16.9 | 40.7 | 8.9 | 29.4 |
| 1989/1990 | 149.0 | 3.2 | −38.8 | 9.3 | 9.2 |
| 1990/1991 | 131.0 | 1.6 | −55.2 | 9.6 | 4.3 |
| 1991/1992 | 329.7 | 10.5 | 134.7 | 9.8 | 28.4 |
| 1992/1993 | 259.9 | 9.1 | 66.1 | 9.8 | 31.5 |
| 1993/1994 | 218.8 | 7.5 | 26.7 | 10.0 | 13.5 |
| 1994/1995 | 234.5 | 14.1 | 35.8 | 10.1 | 22.6 |
| 1995/1996 | 186.2 | 3.1 | −1.6 | 10.2 | 8.7 |
| 1996/1997 | 169.8 | 3.3 | −18.2 | 10.3 | 7.5 |
| 1997/1998 | 185.4 | 2.6 | −1.9 | 10.3 | 6.7 |
| 1998/1999 | 249.9 | 15.0 | 50.3 | 10.8 | 11.0 |
| Average for 15 a | 223.0 | 8.6 | 29.8 | 9.5 | 20.4 |

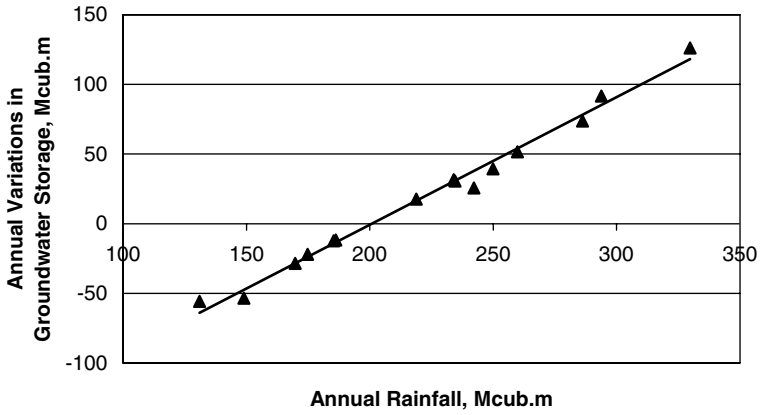


Fig. 6. Regression between annual rainfall and variations in groundwater storage for the entire Kouris catchment for the years 1984–1999.

measured annual rainfall amounts for the period 1978–1983.

The recharge zonation was kept identical to that of the steady-state model. It incorporated a gradual increase of recharge with altitude and dependence on the geology – comparatively low recharge was imposed in the sedimentary complex (Fig. 7). For the years in which evapotranspiration exceeds recharge, net evapotranspiration in the river valleys was input (Fig. 7(b)). Zones of evapotranspiration shown in Fig. 7(b) correspond to a shallow groundwater table in the vicinity of the rivers – in these places the evapotranspiration is highest and occurs during the whole season (Boronina et al., 2005b).

The model was calibrated against transient piezometric observations in boreholes, river baseflows, and spring discharges. The main calibrated parameter was the average storage coefficient. The model showed that only a high storativity led to a satisfactory agreement between observed and simulated piezometric heads. The resulting storage coefficients were the following: 0.0025 for the first layer (from the top), 0.0015 for the second, 0.005 for the third and 0.01 for the fourth. The storage coefficient of the third layer was estimated from the pumping test conducted in Gabbro, while a high value in the fourth layer was due to its large (more than 500 m) thickness.

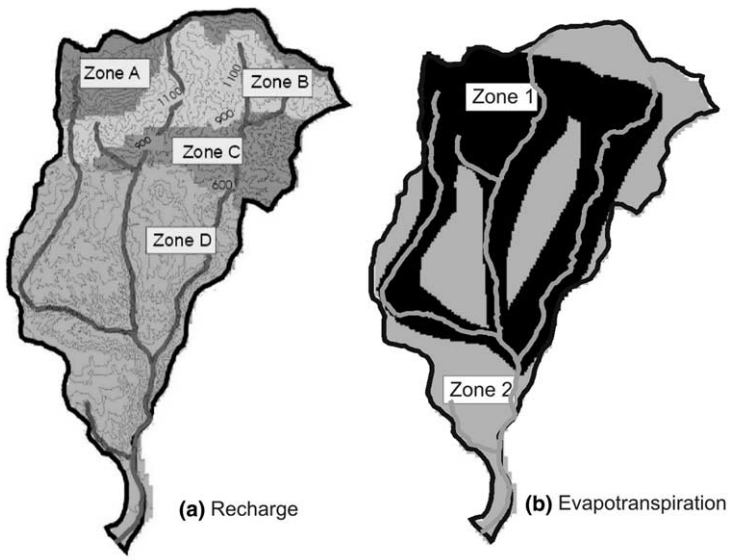


Fig. 7. Time-dependent input parameters for the transient groundwater flow model: (a) recharge; (b) evapotranspiration (Zone 2 refers to no evapotranspiration for all time periods).

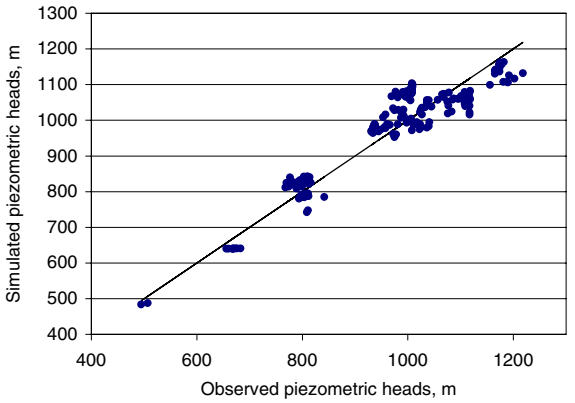


Fig. 8. Scatter diagram of 210 observed and simulated transient piezometric heads for the basic variant.

Fig. 8 shows the scatter diagram of the 210 simulated against the observed transient piezometric heads in 29 boreholes. Discrepancies between measured and simulated values did not exceed 100 m, which was the a priori expected accuracy for such a model in the Kouris catchment (Boronina et al., 2003). The calculated transient variations of the piezometric heads in boreholes satisfactorily agree with observations – see Fig. 9 for two examples.

To obtain these results, recharge and evapotranspiration of extreme (“wet” and “dry”) years had to be slightly smoothed. That was an incorporation of the idea that evapotranspiration (and, consequently, recharge as a residue of the water balance after evapotranspiration – Eq. (5)) is dependent on the amount of water available in soil.

The comparison of modelled baseflows and those derived from hydrograph separation is presented in Fig. 10. The basic variant shows only a weak agreement with the annual baseflow estimated from hydrograph separation (Table 3): the simulated baseflows were considerably smoother. Although the simulated baseflow could be improved (Fig. 10) by halving the storativity, it deteriorates the match between observed and

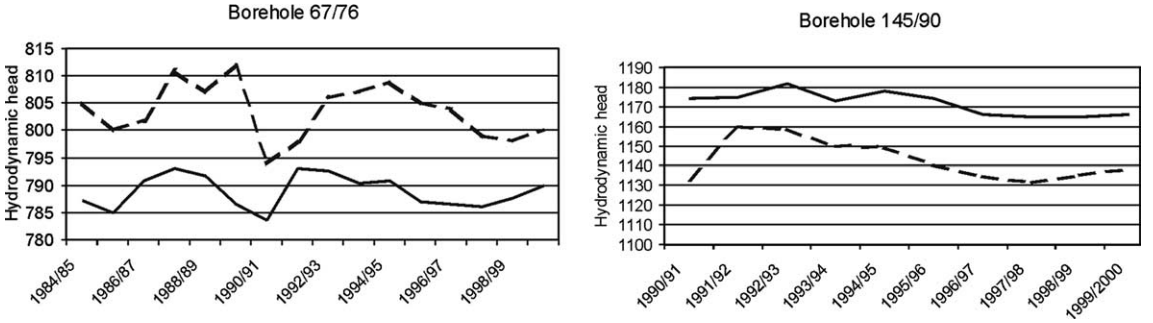


Fig. 9. Examples of comparison between observed (solid lines) and simulated (dashed lines) transient piezometric heads for the boreholes 67/76 and 145/90.

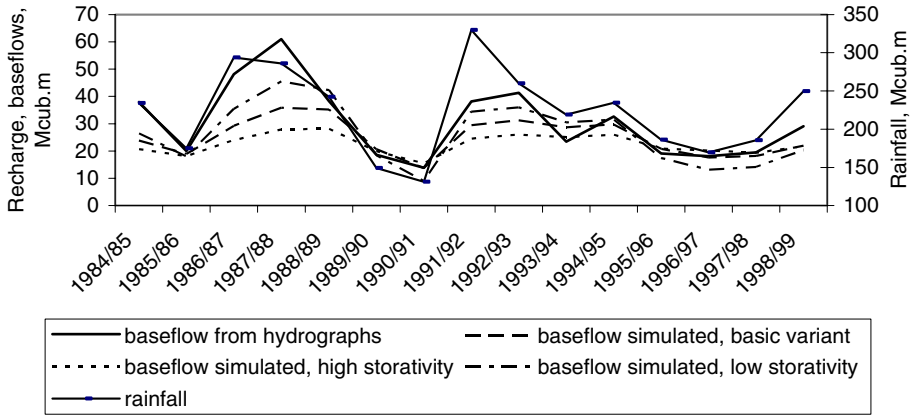


Fig. 10. Comparison of transient baseflows, separated from hydrographs, with those simulated by the numerical models with different input storativities.

simulated piezometry. Doubling storativities slightly improves the simulation of the piezometry, but further smoothes the peaks of simulated baseflows (Fig. 10). Finally, the basic variant, with a total regional storativity of 0.019, was kept as a compromise between baseflow and piezometry calibration; possible causes of the disagreement are discussed below (Section 8).

## 7. Model of tritium transport in the Aquifer

The aim of modelling was to reproduce the $^{3}H$ concentrations in groundwater discharging from springs in the ophiolites in the "dry" seasons of the years 1976–1977 and 1998–1999 (see Fig. 11 for the locations of the springs). All data from rainy seasons were eliminated from the calibration procedure in order to avoid modelling coupled surface/groundwater flow. The authors did not use either analysis from the alluvium aquifer or any data from the boreholes because the first were mixtures of streamwater and groundwater, while the second were associated with different and unknown depths and pumping histories. Thus, $^{3}H$ transport in the aquifer was simulated up to a certain depth (approximately 100 m) related to the vertical size of spring catchments.

The PMPATH advective transport model (Chiang and Kinzelbach, 2001) implying a semi-analytical particle tracking scheme (Pollock, 1988, 1989) was used to simulate particle movement backward from spring cells to recharge areas. The advective transport was modelled on the transient velocity distribution retrieved from the flow model presented above. The assumption of advective transport was, in the authors' opinion, logical, because dispersion along a single flowpath for the studied area should be suppressed by a macro-dispersion due to different lengths of flowpaths from recharge areas to springs. In every spring cell, 30 particles were injected on two circles having a radius of 50 m: one at 3 and one at 6 m below the top of the third layer. Further increase of the number of particles did not change the final distributions of flowpaths.

The results of simulation were simulated flowpaths of the particles for all the springs and residence times along the flowpaths. The calibrated parameters included porosities of the aquifer and the unsaturated zone, and their thicknesses.

The transient $^{3}H$ concentrations were calculated for the years 1976–1977 and 1998–1999 from the simulated PMPATH residence times along all flowpaths and from the $^{3}H$ input function, accounting for the radioactive decay. The input function uncertainties were propagated to estimate the simulated $^{3}H$ concentration uncertainties. Those were rather high for some years (for example, 20 TU for the groundwaters having a residence time of 10 a and sampled in 1976).

A scatter diagram of observed versus simulated $^{3}H$ concentrations is presented in Fig. 12. This variant was simulated with the final set of calibrated parameters (Table 4). The simulated residence times in springs sampled in 1998/1999 are shown in Table 5. Mean residence times were sensitive to a relevant period: in 1998, after several extreme "dry" years, they were higher than in 1976. Fig. 13 shows as an example, the transfer function simulated with PMPATH for the Archolochania spring. Generally, for the modelled springs, the simulated transfer functions were of the piston or dispersion types with different macro-dispersivity values.

The resulting concentrations were rather sensitive to a $^{3}H$ content of groundwater arriving via a single

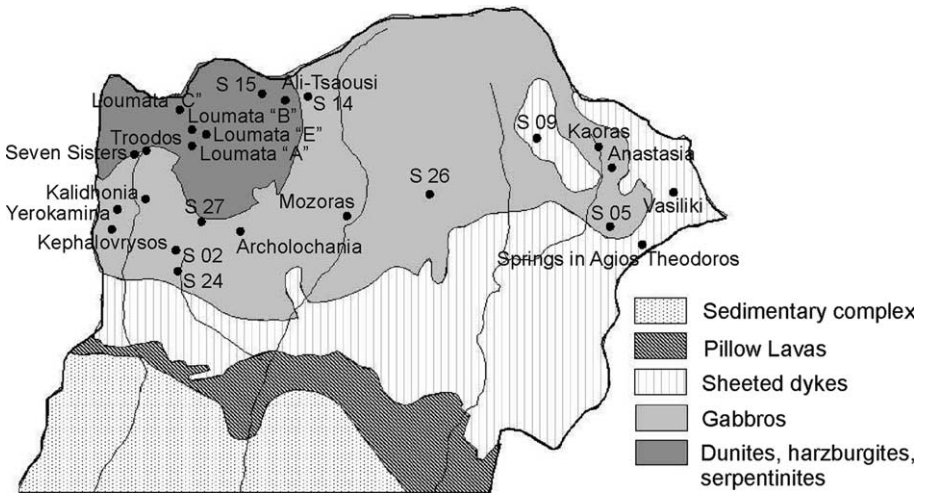


Fig. 11. Location of springs included in the numerical model of $^{3}H$ transport.

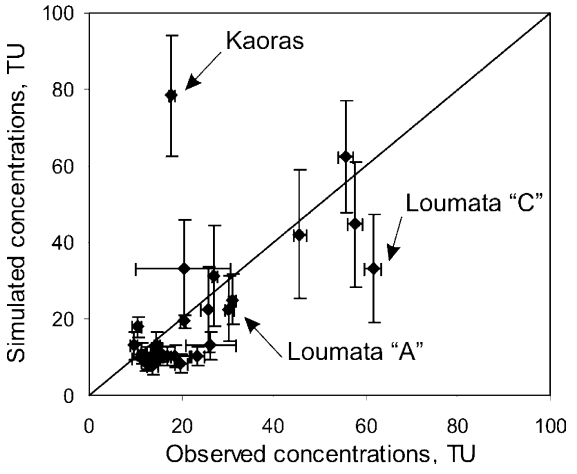


Fig. 12. Scatter diagram between observed and simulated $^{3}H$ concentrations (best fit) with the uncertainty ranges.

flowpath, while this did not influence mean residence times. Thus, 19–20 a of mean residence time can be associated with a whole range of concentrations from 30 to 130 TU in 1976–1977. For samples taken in 1998, it was enough to have two flowpaths with residence times of 36 a, which does not change the average residence time (19–20 years), but takes the simulated concentration in springs from 7 to 13 TU. This explains why it is difficult to achieve a good fit between observed and simulated $^{3}H$ concentrations although even quite large differences between single values (when they are normally distributed) still result in correct mean residence times.

The resulting concentrations and the residence times were rather sensitive to porosities of the ophiolitic aquifer and unsaturated zone. The optimal porosities, derived from model calibration, were between 0.04 and 0.06 (Table 4, Fig. 12). Increasing or reducing porosities by a factor of 3, results in unacceptable $^{3}H$ concentrations (Fig. 14).

Table 5
Simulated residence times (in years) for the selected springs of ophiolitic complex

| Spring name | Min. residence time | Max. residence time | Average residence time of distribution |
|---|---|---|---|
| Loumata "A" | 18 | 31 | 23.4 |
| Loumata "B" | 18 | 23 | 20.0 |
| Loumata "C" | 18 | 27 | 21.2 |
| Loumata "E" | 17 | 18 | 17.9 |
| Troodos (Spring 21A,B,C) | 18 | 41 | 22.5 |
| Seven Sisters | 18 | 23 | 19.8 |
| Kalidhonia | 18 | 20 | 18.9 |
| Yerokamina | 18 | 20 | 19.4 |
| Kephalovrysos (at P. Platres) | 17 | 23 | 20.4 |
| Spring 02 | 17 | 20 | 18.2 |
| Spring 24 | 17 | 22 | 19.1 |
| Spring 27 | 18 | 18 | 18.0 |
| Archolochania | 18 | 30 | 21.4 |
| Mozoras | 20 | 31 | 25.2 |
| Spring 15 | 18 | 31 | 21.9 |
| Ali-Tsaousi | 18 | 27 | 21.1 |
| Spring 14 | 17 | 20 | 19.0 |
| Spring 26 | 30 | 31 | 30.5 |
| Vasiliki | 13 | 17 | 14.2 |
| Spring 04, Spring 05 | 17 | 26 | 21.3 |
| Springs at Agios Thodoros | 13 | 16 | 14.1 |
| Anastasia | 13 | 32 | 22.0 |
| Kaoras | 13 | 17 | 14.3 |
| Spring 09 | 17 | 27 | 21.8 |

Table 4
Input parameters for PMPATH model for the ophiolitic complex as a result of model calibration

| Calibrated parameter | Min. value for ophiolites | Max. value for ophiolites |
|---|---|---|
| *Transmissivity ($m^2$/day)* | | |
| Lower layer of the aquifer | 3.6 | 12.9 |
| Upper layer of the aquifer | 0.9 | 3.2 |
| *Vertical hydraulic conductivity of the unsaturated zone (m/day)* | 0.5 | 0.5 |
| *Porosity* | | |
| Aquifer (both layers) | 0.05 | 0.06 |
| Lower layer of the unsaturated zone | 0.05 | 0.05 |
| Upper layer of the unsaturated zone | 0.09 | 0.11 |
| *Thickness (m)* | | |
| Lower layer of the aquifer | 40 | 40 |
| Upper layer of the aquifer | 10 | 10 |
| Lower layer of the unsaturated zone | 20 | 60 |
| Upper layer of the unsaturated zone | 10 | 10 |

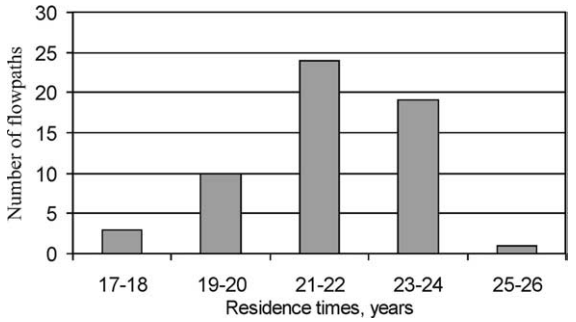


Fig. 13. Distribution of residence times for Archolochania spring for September 1976 with 27.5 TU and the average residence time 21.9 a.

Fig. 15 shows the simulated groundwater flowpaths for the main springs of the ophiolitic complex; it is seen that the spring catchments had lengths up to 5 km originating in areas of higher recharge. They were narrow in shape as a consequence of the regional piezometric field controlled by the river valleys. This fact must be taken into account when planning protection zones for the springs when used as drinking water supplies.

## 8. Discussion

### 8.1. Modelling of transient groundwater flow

The models calibrated against borehole piezometry and streamflow resulted in different values for the calibrated storativities. In the authors' opinion, there are, at least, two possible reasons for that contradiction.

*Overestimation of baseflows calculated from hydrographs for extreme "wet" years.* In Cyprus, large amounts of rainfall are often caused by intensive rains rather than by a large number of rainy days. In the case of rainfall intensity exceeding infiltration capacity, water drains to the rivers without infiltration in the deep aquifer. One assumption underlying the hydrograph separation method is complete cessation of surface runoff within two days following the precipitation (Sloto and Crouse, 1996). Thus, the baseflows simulated by the

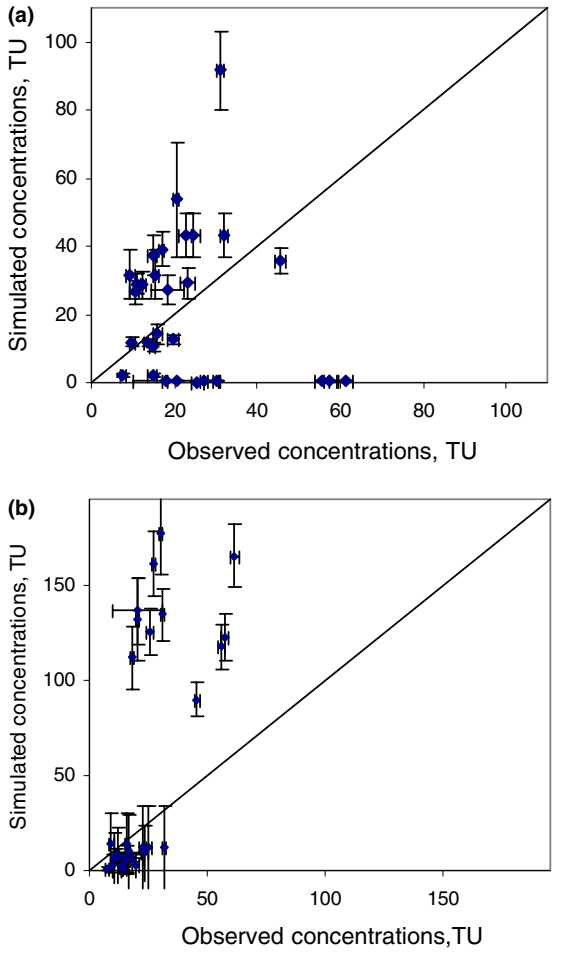


Fig. 14. Scatter diagram between observed and simulated $^{3}H$ concentrations: (a) variant with "high" input porosity; (b) variant with "low" input porosity. Bars represent uncertainty of observed and simulated values, respectively.

Fig. 15. Delineation of several spring catchments in the ophiolitic complex with PMWIN.

numerical model might be more realistic for "wet" years than those obtained from hydrograph separation. Note that the baseflows during "dry" or average years obtained from hydrograph separation were pretty similar to those obtained from the numerical model (Fig. 10).

*Different storage parameters, controlling baseflow and piezometry variations*. In the Kouris catchment, boreholes were drilled selectively in the most productive zones and often showed unconfined conditions during operation. On the other hand, baseflow mainly originates from ophiolitic springs in the upper part of the catchment, where the specific storage is smaller (the idea of "mountain origin" of the baseflow is also supported by the stable isotope studies – Boronina et al. (2005a)). Thus, baseflow seemed to represent regional storage of the upper part of the ophiolitic aquifer, while piezometric heads in boreholes were more related to local areas under an artificially unconfined regime.

### 8.2. Modelling of $^3H$ transport in the aquifer

The $^3H$ transport was simulated for the upper part of the ophiolitic aquifer (up to 100 m deep) associated with the largest regional springs. Consisting of typically plutonic and intrusive rocks, the aquifer is highly heterogeneous in permeability and porosity. Consequently, it was difficult to calibrate the regional model against local data from a spring by adjusting only averaged hydrogeological properties.

Thus, an acceptable simulation for the Kaoras spring under this regional assumption was not achieved (Fig. 12) – it is proposed that this spring should be studied separately in the future especially because, it is an important water resource for Agros village, and already contaminated by sewage.

Similarly the spring Loumata "C" could not be modelled properly. Indeed, the springs Loumata "A" and Loumata "C" (Fig. 11) are located at a distance of 200 m from each other (less than 2 model cells) and both flow from outcrops of similar rock types (harzburgites). However, in September 1976, they discharged water with very different $^3H$ contents: 30.3 TU for Loumata "A" and 61.5 TU for Loumata "C". Such differences cannot be modelled under regional assumptions.

Nevertheless, modelling all those springs with the numerical model was still important because it provided essential information about the regional hydrogeological properties of the ophiolites. Furthermore, the modelling allowed the authors to distinguish the springs behaving mainly according to regional constraints from those controlled by more local properties.

An important finding was the value of the regional porosity of the ophiolites estimated to be 0.05–0.06 as a result of the transport model calibration. Despite a large uncertainty of the results and a high scatter between observed and simulated concentrations, the estimated range of porosities is quite narrow (Figs. 12 and 14). The rather high value that was estimated for fracture porosity suggests involvement of the rock matrix porosity in $^3H$ transport.

The fact that the groundwater flow model could not be used to reproduce $^3H$ concentrations in an aquifer with calibrated porosities that looked realistic, justifies, in a certain way, the assumptions and input data set for the flow model. However, it was not possible to use $^3H$ data directly for calibration of the groundwater flow model. Generally, advective transport models allow calibrating only actual velocities that result from input transmissivities, porosities, recharge and other boundary conditions. In the present study, the authors preferred to keep constant flow parameters (that were already results of the calibrated flow models) and to calibrate porosities.

To simulate $^3H$ transport, a groundwater flow model was chosen with a storage coefficient 0.019 (basic variant) that represented regional storage properties of the ophiolitic aquifer rather than local zones around boreholes. Disagreement of baseflows simulated and calculated from curve-fiting methods for extreme "wet" years are related to inaccuracy of the curve fitting methods more than to wrong modelling assumptions. However, varying storage coefficient at the range 0.009–0.038 only a negligible influence on results of transport simulations compared to transient variations of recharge.

## 9. Conclusions

Seventy seven historic $^3H$ analysis from Jacovides (1979) and 176 recent ones in the Kouris catchment allowed the construction of an input function of $^3H$ content in precipitation and obtaining essential hydrogeological information about the aquifer.

The groundwaters in the sedimentary aquifer and Pillow Lavas had residence times of more than 48 a; thus they were considerably "older" than the groundwater of the ophiolitic complex. Even in the vicinity of the rivers, the sedimentary complex contained water with low $^3H$ content, indicating that the sedimentary aquifer was probably receiving no water infiltrated from the rivers. The groundwaters in the river alluvium had $^3H$ contents very similar to the river water, and rather different from the groundwater of the surrounding sediments. The biggest springs in the southern part of the catchment, located in river valleys, were discharging groundwater similar to those in the rivers and in the alluvial aquifer.

Low $^3H$ contents (less than 1 TU) were observed in groundwater of deep boreholes of the ophiolitic complex, exploited for irrigation during "dry" seasons. This

shows that those boreholes were pumping water having a long period of renewal.

The transient groundwater flow model showed contradictions between storage coefficients calibrated against baseflow, and those calibrated against piezometric data from boreholes. Baseflow variations seemed to be controlled by the regional storage parameters of the upper part of the ophiolitic aquifer, while transient water levels in the boreholes are controlled by local permeable areas.

The simulation of $^{3}H$ transport in the aquifer was performed with the PMPATH transient model. The average residence times of spring water in the ophiolitic complex were estimated to be between 14 and 30 a, although a few springs could not be modeled adequately with the regional model. The porosities of the aquifer and the unsaturated zone were estimated to be between 0.05 and 0.11. The PMPATH model also allowed for the delineation of the main spring catchments, which were narrow zones of up to 5 km length.

## Acknowledgments

The authors thank W. Kinzelbach for helpful discussions and F. Leuenberger for correcting the draft of this paper. We are very grateful to colleagues from the Water Development Department of Cyprus for their support in field work. The research was financially supported by ETH, Zuerich (Internal Research Project TH-22./01-1).

## References

Afrodisis, S., Avraamides, C., Fischbach, P., Hahn, J., Udluft, P., Wagner, W., 1986. Hydrogeological and hydrochemical studies in the Troodos region, Technical Report N6 in Cyprus-German Geological and Pedological Project No. 81.2224.4, Ministry of Agriculture and Natural Resources, Geological Survey Department, Nicosia, Cyprus.

Boronina, A., Renard, P., Balderer, W., Christodoulides, A., 2003. Groundwater resources in the Kouris catchment (Cyprus): data analysis and numerical modelling. J. Hydrol. 271, 130–149.

Boronina, A., Balderer, W., Renard, P., Stichler, W., 2005a. Study of stable isotopes in the Kouris catchment (Cyprus) for the description of the regional groundwater flow. J. Hydrol. (in press).

Boronina, A., Golubev, S., Balderer, W., 2005b. Estimation of actual evapotranspiration from an alluvial aquifer of the Kouris catchment (Cyprus) using continuous streamflow records. Hydrol. Proc. (in press).

Chiang, W.-H., Kinzelbach, W., 2001. 3D Groundwater Modeling with PMWIN. Springer, Berlin.

Harbaugh, A.W., McDonald, M.G., 1996. User's Documentation for Modflow-96, an Update to the US Geological Survey Modular Finite-Difference Ground-Water Flow Model.

Jacovides, J., 1979. Environmental isotope survey (Cyprus), Final Report on I.A.E.A., Research Contract No: 1039/RB, Technical Report, Ministry of Agriculture and Natural Resources, Department of Water Development, Nicosia, Cyprus.

Jorin, U., 2001. Geologische und hydrogeologische Untersuchungen zu den Grundwasservorkommen des Troodos-Ophioliths im Einzugsgebiet des Yermasoyia River. Diploma Thesis, Geologisches Institut, ETH Zuerich.

Kitching, R., Edmunds, W.M., Shearer, T.R., Walton, N.R.G., Jacovides, J., 1980. Assessment of recharge to aquifers. In: Hydrol. Sci. – Bull Sci. Hydrologiques 25,3,9, pp. 217–235.

Konikow, L.F., 1996. Numerical models of groundwater flow and transport. In: Manual on Mathematical Models in Isotope Hydrology, IAEA-TEC-DOC-910, Vienna, Austria, pp. 59–112.

Maloszewski, P., 1996. Lumped parameter models for the interpretation of environmental tracer data. In: Manual on Mathematical Models in Isotope Hydrology, IAEA-TEC-DOC-910, Vienna, Austria, pp. 9–58.

Maloszewski, P., Zuber, A., 1982. Determining the turnover time of groundwater systems with the aid of environmental tracers, I – models and their applicability. J. Hydrol. 57, 207–231.

Marechal, J.C., Etcheverry, D., 2003. The use of $^{3}H$ and $^{18}O$ tracers to characterize water inflows in Alpine tunnels. Appl. Geochem. 18, 339–351.

Moll, A., 2000. Hydrogeologie des Einzugsgebietes des Kouris und der Gegend von Agros (Zypern). Diploma Thesis, Geologisches Institut, ETH Zuerich.

Pettyjohn, W.A., Henning, R., 1979. Preliminary estimate of ground-water recharge rates, related streamflow and water quality in Ohio, Project Completion Report 553. Technical Report, Columbus, Ohio State University, Water Resources Centre.

Plummer, L.N., Busenberg, E., Bohlke, J.K., Nelms, D.L., Michel, R.L., Schlosser, P., 2001. Groundwater residence times in Shenandoah National Park, Blue Ridge Mountains, Virginia, USA: a multi-tracer approach. Chem. Geol. 179, 93–111.

Pollock, D.W., 1988. Semianalytical computation of path lines for finite difference models. Ground Water 26, 743–750.

Pollock, D. W., 1989. MODPATH (version 1.x), Documentation of computer programs to compute and display pathlines using results from the US Geological Survey modular three-dimensional finite-difference ground-water model. US Geol. Surv. Open-file Rep. 89–381.

Sloto, R.A., Crouse, M.Y., 1996. HYSEP: a computer program for streamflow hydrograph separation and analysis, Water-Resour. Investig. Rep. 96-4040, US Geol. Surv., Lemoyne, Pennsylvania.

Steiner, M., 2000. Geologische und hydrogeologische Untersuchungen im Einzugsgebiet des Kouris River (Zypern). Diploma Thesis, Geologisches Institute, ETH Zuerich.

Stimson, J., Rudolph, D., Frape, S., Drimmie, R., 1996. Interpretation of groundwater flow patterns through a reconstruction of the tritium precipitation record in

the Cochabamba Valley, Bolivia. J. Hydrol. 180, 155–172.

Verhagen, B.T., Geyh, M.A., Fröhlich, K., Wirth, K., 1991. The Lefkara area, Cyprus. In: Isotope Hydrological Methods for the Quantitative Evaluation of Ground Water Resources in Arid and Semi-arid Areas. Research Reports of the Federal Ministry for Economic Cooperation of the Federal Republic of Germany, Bonn, Germany, pp. 43–59.

Zuber, A., 1986. Mathematical modelling for the interpretation of environmental radioisotopes in groundwater systemsHandbook of Environmental Isotope Geochemistry, vol. 2. Elsevier, Amsterdam.